Hydrogen-Deficient Stars
ASP Conference Series, Vol. 391, © 2008
K. Werner and T. Rauch, eds.

Hydrogen-Deficient Compact Pulsators: The GW Virginis Stars and the Variable DB White Dwarfs

Pierre-Olivier Quirion

Institut for Fysik og Astronomi, Aarhus Universitet Ny Munkegade, Bygn. 1520, 8000 Århus-C, Denmark

Marc-Antoine Dupret

Observatoire de Paris, LESIA, CNRS UMR, 8109, 5 place J. Janssen, 92195 Meudon, France

Gilles Fontaine and Pierre Brassard

Département de Physique, Université de Montréal, C.P. 6128, Succ. Centre-Ville, Montréal, Québec, Canada H3C 3J7

Ahmed Grigahcène

CRAAG - Algiers Observatory, BP 63, Bouzareah 16340, Algiers, Algeria

Abstract. We review briefly the basic properties of the GW Vir stars and of the V777 Her stars. We describe the classical κ-mechanism operating in the GW Vir stars and the effects of the chemical composition and of the interaction between diffusion and mass loss on the boundaries of the instability domain of these objects in the $\log g - T_{\rm eff}$ diagram. Because of the presence of an extensive superficial convection zone in pulsating DB (V777 Her) white dwarfs, oscillation modes are not excited through a similar classical κ-mechanism in those stars but, instead, involve pulsation-convection interactions. We describe the effects of a time-dependent convection (TDC) treatment on the driving mechanism of the V777 Her stars. We show how convection deeply affects the excitation of modes via the entropy transport mechanism or S-mechanism. Provisional blue and red edges are calculated for the V777 Her stars and are found at $T_{\rm eff} \simeq 28,500$ K and $\simeq 20,500$ K, respectively, for a 0.6 $M_\odot$ star under the assumption of ML2 convection.

1. GW Vir Stars

The GW Vir stars constitute a class of pulsating stars concentrated in the region connecting the post-Asymptotic Giant Branch (post-AGB) stars and the white dwarfs in the HR diagram. This region spans wide ranges covering $5.5 \lesssim \log g \lesssim 7.5$ and $80,000$ K $\lesssim T_{\rm eff} \lesssim 170,000$ K. The GW Vir stars show multi-periodic luminosity variations caused by low-degree, intermediate-order g-mode oscillations. These oscillations are driven by a classical κ-mechanism caused by the partial ionization of K-shell electrons in carbon and oxygen. Their observed periods are found in the range from 300 s to upward of 5000 s.

One of the many peculiar aspects of GW Vir stars is that they enclose many spectroscopic classes. PG 1159 stars, early-type Wolf-Rayet central stars of planetary nebulae (early-[WC] or [WCE]), and their subtypes (hybrid PG 1159 stars and [WC]-PG1159 transition objects) can all show luminosity variations of the GW Vir type (Quirion et al. 2007a). As discussed in the excellent review paper presented recently by Werner & Herwig (2006), quantitative spectroscopy and detailed evolutionary calculations imply very strongly a tight evolutionary connection following the sequence [WCE]→PG 1159. Winds produce wide carbon emission lines in [WC]-type stars, giving them their characteristic spectral signature. With time and decreasing luminosity, the magnitude of the outgoing wind diminishes, thus weakening the carbon emission lines in such evolved stars. This ultimately leads to the specific PG 1159 features to appear in the spectra of the newly-born [WC]-PG 1159 transition object. A further decrease of the wind magnitude completes this scenario whereby the wide carbon emission lines disappear. The star now has a full characteristic PG 1159 spectrum.

The general picture on mass loss has been summarized by Werner (2001). Winds reaching magnitudes of 10^{-5} to $10^{-6.5}$ $M_{\odot}$ yr^{-1} and decreasing with proceeding post-AGB evolution characterize the [WC] stars. A mass loss rate of 10^{-7} $M_{\odot}$ yr^{-1} has been estimated in two [WC]-PG 1159 transition objects, and a value of 10^{-7} to 10^{-8} $M_{\odot}$ yr^{-1} has been found in one low-gravity PG 1159 star. With these relatively high values of the mass loss rate, it is expected that the envelope composition of all these very hot stars is essentially uniform and homogeneous (see Chayer et al. 1997; Unglaub & Bues 2000, 2001). Because of the homogeneity of the envelopes, the observed atmospheric abundances must reflect the chemical composition in the deeper layers where mode driving occurs. In all cases involving GW stars, the driving is related to the cyclic ionization of the K-shell electrons in carbon and oxygen, the two main atmospheric constituents in these stars along with helium (see Werner & Herwig 2006). The positions of the 18 known GW Vir stars in the $\log g - T_{\rm eff}$ diagram along with their spectral identifications are shown in Figure 1.

This figure summarizes our actual knowledge of the shape of the instability domain for GW Vir stars. A recent detailed study of the κ-mechanism and of the blue edge(s) of the instability strip has been presented in Quirion et al. (2007a). It is shown there that different GW Vir envelope chemical compositions lead to different blues edges. A general rule states that stars with higher contents of carbon and oxygen tend to have a blue edge at higher temperatures. Since the carbon and oxygen contents vary from star to star, the blue edge is necessarily "fuzzy", and is represented here by the multiple dotted lines of Figure 1. If we look at the path taken by the representative 0.6 $M_{\odot}$ evolutionary model, we note that a star evolving through the GW Vir region may go through the instability strip twice during its excursion in that part of the HR diagram.

Figure 1 also shows three different theoretical red edges. The positions of the red edges are tightly linked to the transformation of PG 1159 stars into DO white dwarfs. The evolutionary connection following the sequence PG 1159→DO, where the spectral type DO belongs to He-dominated atmosphere white dwarfs, is strongly supported by quantitative spectroscopy (Werner & Herwig 2006). The strong wind present in [WC] and PG 1159 stars tends to homogenize their envelope, but as this wind weakens along with decreasing luminosity, it progressively looses its homogenizing capacity. Gravitational settling then takes

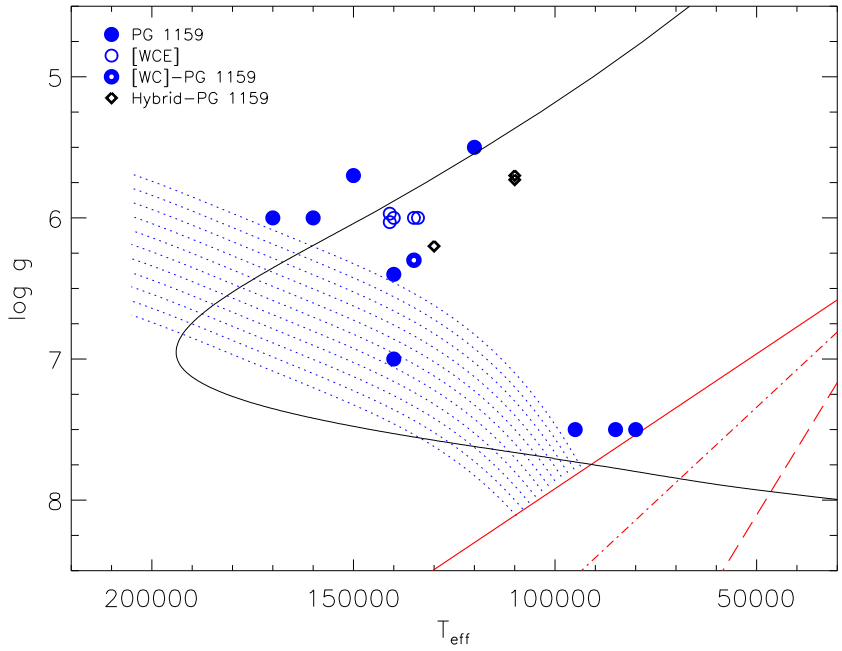

Figure 1. Positions of the GW Vir stars in the $\log g - T_{\rm eff}$ diagram. The different spectral types are specified by different symbols. The dotted curves symbolize the intrinsic fuzziness of the blue edge caused by its dependence on the atmospheric chemical composition. The three straight lines are the theoretical red edges calculated with full evolutionary models including diffusion and mass loss. Each red edge is calculated with a different mass loss law, $\dot{M} = 1.00 \times 10^{-17} L^{2.36}$ refers to the solid line, $\dot{M} = 1.29 \times 10^{-15} L^{1.86}$ refers to the dot-dashed line and $\dot{M} = 1.82 \times 10^{-13} L^{1.36}$ refers to the dashed line.

over, causing carbon and oxygen to sink below and helium to float at the surface of the star. As carbon and oxygen are responsible for the mode driving via the κ-mechanism, their gravitational settling will ultimately stop the stellar oscillations, drawing the red edge of the GW Vir class.

The three red edges of Figure 1 were derived using full evolutionary calculations including diffusion and mass loss (Quirion et al. 2007b). The models are purely radiative at each time step. Convection plays no role in the structure and in the stability analysis of GW Vir stars. Each red edge corresponds to a different mass loss law used in the evolutionary calculations. A weaker mass loss leads to faster gravitational settling and, therefore, to a red edge located at a higher temperature, while a stronger mass loss keeps carbon and oxygen

mixed with helium for a longer period of time and moves the red edge at a lower effective temperature.

Unfortunately, and despite observed evidence of stellar winds in evolved PG 1159 and DO stars (see Dreizler et al. 1995, for evidence of winds in DO white dwarfs), many unknowns related to the lack of theoretical understanding of the mass loss process in these compact stars must still be addressed. The description of the mass loss recipes used in the calculations presented here, as well as details on the cooling process leading to the red edge, is given in Quirion (2007) and in Quirion et al. (2007b).

The scenario of a GW Vir star reaching the red edge is presented in Figure 2. We chose four models along our 0.6 $M_{\odot}$ evolutionary track, under the effect of diffusion and mass loss. The magnitude of the mass loss is $\dot{M} = 1.29 \times 10^{-15} L^{1.86}$ ($M_{\odot}$ yr^{-1}). The figure represents, in a chronological way, the evolution of the internal structure of our model, the formation of the red edge, and the transformation of our PG 1159 model into a DO star. We see that, as the star cools down, the carbon and oxygen abundances in its driving/damping layers – the driving/damping layers are the ones where the dynamical and thermal time scales are of the same order, where the oscillations are excited and damped – get lower. This reduction leads to a smoothing of the opacity bump created by the partial ionization of C and O. This make the κ-mechanism less and less efficient. The red edge is found between the 69,877 K and the 67,865 K models. It is interesting to note that the last unstable model, at 69,877 K, shows only a small amount of carbon and essentially no oxygen at its surface with $X(\mathrm{He}) \simeq 0.97$ and $X(\mathrm{C}) \simeq 0.03$. This composition ratio would prevent a GW Vir star with a strictly uniform envelope composition to be unstable. However, the composition gradient created by diffusion in the envelope can lead, in these very late phases of GW Vir evolution, to stellar instability. The discovery of a GW Vir star with very low amounts of carbon and oxygen would be a tracer of diffusion activity. The coolest model, stable at 44,694 K, has been transformed into a DO white dwarf. Indeed, helium completely fills the envelope from the surface of the star down to $\log q \sim -7.0$. The residual opacity bump at $\log q \sim -6.0$ only marks the transition from the pure helium surface to a He/C/O mixture underneath, far below the potential driving/damping layers.

2. Pulsating DB White Dwarfs

The V777 Her or variable DB white dwarfs (DBV) are the helium-rich analogs of the better know hydrogen-rich ZZ Ceti stars. They show multiperiodic g-mode oscillations with typical periods between 200 and 1000 seconds. Beauchamp et al. (1999) have shown that their effective temperatures and surface gravities are subject to uncertainties caused by the possible presence of undetectable hydrogen in their atmospheres. Voss et al. (2007) have shown, using high-resolution VLT spectra, that at least $\sim 50\%$ of the DB white dwarfs are actually showing hydrogen traces. Figure 3 shows the possible positions related to unknown hydrogen traces of the pulsating DB white dwarfs in the $\log g - T_{\mathrm{eff}}$ diagram. Because of this large influence of the hydrogen traces, the empirical instability strip of the V777 Her stars is, unlike the ZZ Ceti stars, expected to be polluted by stable white dwarfs.

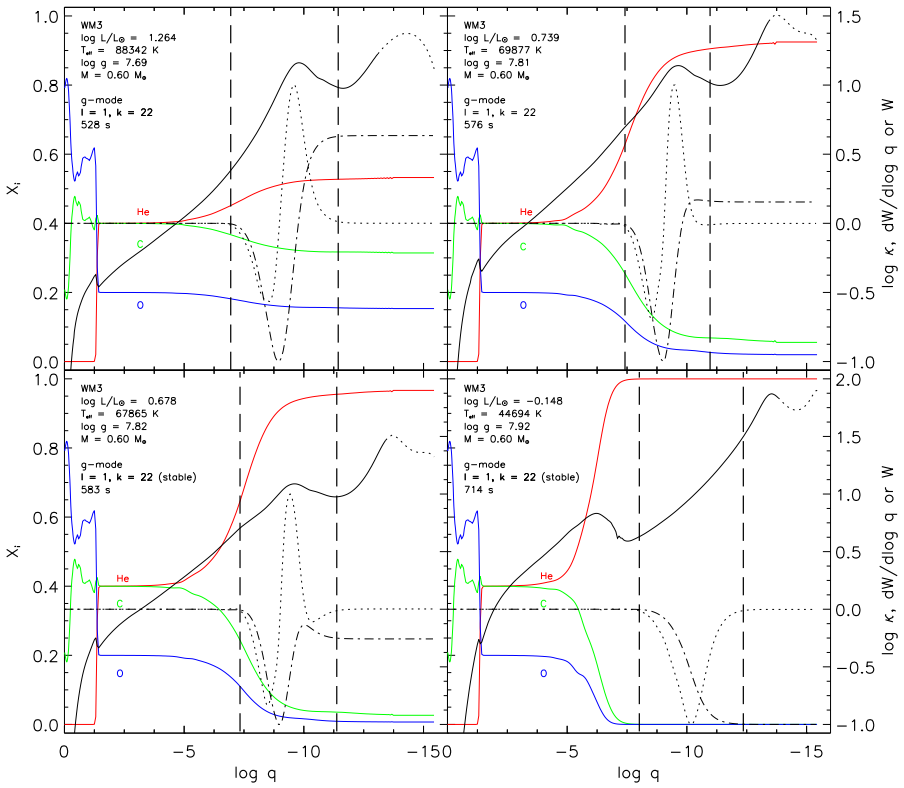

Figure 2. Four models taken along a 0.6 $M_\odot$ track showing the effects of diffusion on the chemical composition of the envelope of a star undergoing a mass loss of $\dot{M} = 1.29\times10^{-15}L^{1.86}\ M_\odot\ \mathrm{yr}^{-1}$. The composition of the envelope at the start of the calculation was $X(\mathrm{He}) = 0.40$, $X(\mathrm{C}) = 0.40$ and $X(\mathrm{O}) = 0.20$ in mass fractions. The solid curves associated with helium, carbon, and oxygen (in the electronic version: red, green, and blue, respectively) depict the progressive rise of the helium content at the surface, prompted by gravitational settling of carbon and oxygen, as the mass loss decreases with decreasing luminosity. The two models in the top panels, at $T_{\mathrm{eff}} = 88,342$ K and $69,877$ K, are unstable, as shown by the positive value of the work integral W (running from left to right) at the surface of the models. The driving/damping region, defined by the zone between the two vertical dashed lines, indicates where the magnitude of the derivative of the work integral $dW/d\log q$ is greater than 1% of its maximal value (normalized at either +1 or −1). The maximum of the driving occurs, as it is always the case for a classic κ-mechanism, near the maximum of the opacity bump. The bump is seen in the Rosseland opacity κ around $\log q \sim -9.5$. For the two stable models in the lower panels, at $T_{\mathrm{eff}} = 67,865$ K and $44,694$ K, we see negative values of the work integral at the surface of the star along with the vanishing opacity bump. The dotted extensions of the κ curves mark the extent of the atmosphere, defined here as those layers with an optical depth $\tau_{Ross} < 100$.

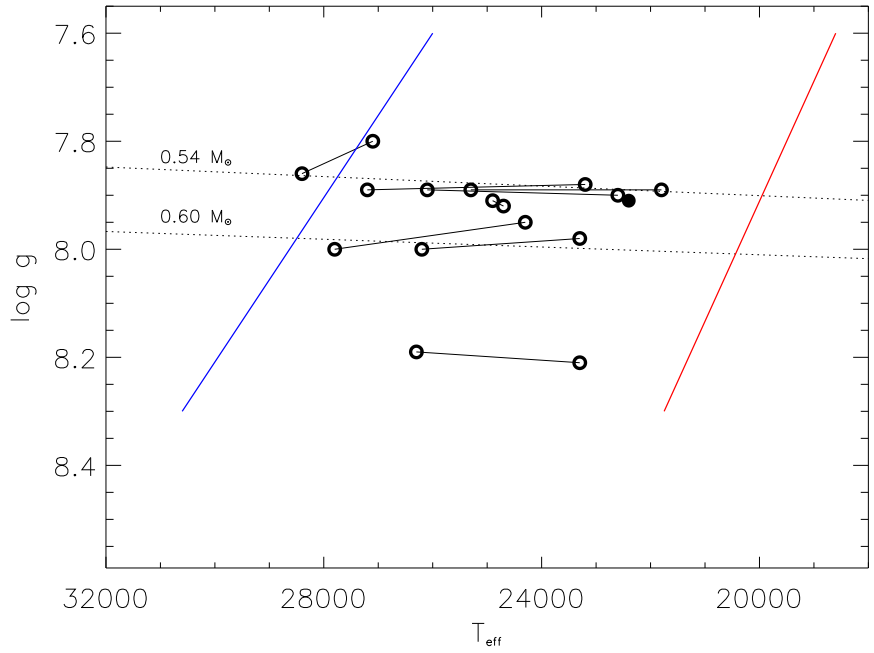

Figure 3. Theoretical instability domain and positions of the V777 Her stars in the $\log g - T_{\rm eff}$ diagram. Two solutions (open circles) are given for those objects with unknown H contents: the left position corresponds to zero H, and the right position to the maximum possible amount just below the detection limit. The filled circle is a pulsating DBA (a DB with a detected trace of hydrogen).

We have calculated two evolutionary tracks for DB white dwarfs with the same white dwarf evolution code used for the GW Vir stars presented in the previous section. No diffusion was included in these particular calculations, however. To model the superficial helium convection zone that develops with cooling, we used the mixing-length theory with the ML2 prescription of Tassoul et al. (1990). We used a pure helium composition from the surface down to a fractional mass depth of $\log q = -2$, where the transition is made to a core composed of carbon and oxygen in equal ratios. We considered a 0.54 and a 0.60 $M_{\odot}$ track to study the DBV strip with the MAD nonadiabatic code (Grigahcène et al. 2005; Dupret 2002). This code includes a time-dependent treatment of convection (TDC). The positions of the derived blue and red edges are shown in Figure 3.

The usual approach to convection in nonadiabatic calculations applied to white dwarfs has been the frozen convection (FC) approximation. The first

exceptions to this standard approach in the field has been the work of Gautschy et al. (1996) and Brassard & Fontaine (1997) where an instantaneous correction to the convective flux is applied to the study of the ZZ Ceti instability strip. In the case of white dwarfs, some aspects of the TDC approach are quasi-equivalent to the instantaneous correction of the convective flux as the convective time scale is much smaller than the observed pulsation periods in white dwarfs (see Figure 4). In contrast, the FC approach assumes that the convection time scale is much larger that the excited periods, $\tau_c \gg P$. We see from Figure 4 that this approximation is not justified. We are, in fact, in the instantaneous regime where $\tau_c \ll P$.

If the instantaneous correction of the convective flux is valid at the blue edge, it is not necessarily justified at lower temperatures. For instance, near $\sim 20,000$ K, at the base of the convection zone, $\tau_c \simeq P$. Under these conditions, only a full TDC approach can be used. Also, the TDC used here includes a perturbation of the turbulent pressure which has not been considered in any of the previous studies. Moreover, a free parameter β is introduced in the closure equation of the TDC treatment (Grigahcéne et al. 2005). The choice of β has no influence on the position of the blue edge. The turbulent pressure is thus not a factor at high temperatures. However, turbulent pressure variations enhanced by a factor of 4 must be included in the models to get the theoretical red edge shown in Figure 3. The effects of the turbulent pressure term on the V777 Her red edge are introduced in Dupret et al. (2008) and will be investigated thoroughly elsewhere. The rest of this section is devoted to the effects of convection around the blue edge.

If we go back to Figure 2, the lower right panel shows that, while the star has been transformed into a helium-rich white dwarf, an opacity bump, at $\log q \sim -14.0$ has started to drift slowly toward the driving/damping layers deeper into the star. This bump is related to the partial ionization of HeII. When the star reaches $T_{\rm eff} = 28,000$ K, the opacity bump has moved down near the driving/damping layers, and becomes the ultimate cause of the DBV instability strip. However, there is a fundamental difference between the standard opacity-driven κ-mechanism, like the one operating in GW Vir stars, and what we have for the V777 Her stars. In Figure 4 we present an unstable 0.54 $M_\odot$ model close to the blue edge. The maximum of the driving is not at the maximum of the opacity bump, but directly at the base of the convective zone.

We call this mechanism present in V777 Her models *entropy transfer* or *S-mechanism*. This transfer is illustrated on Figure 5. We reproduce there the real value of the entropy perturbation δS, of the temperature perturbation δT, and the derivative of the work $dW/d\log q$ for the FC treatment and for the TDC treatment of our 0.54 $M_\odot$ model close to the blue edge. It is worth mentioning that, for this model at $T_{\rm eff} = 26,700$ K, the FC treatment keeps the star stable while the TDC treatment drives pulsations.

Figure 5 shows that the entropy perturbation created by the partial ionization zone, at $\log q \sim -14$ in the FC case, is transported through the convective region in the TDC case. The adiabatic transport at the bottom of the convective zone keeps δS constant there. Continuity makes δS large in a narrow zone just below the convective layers, where it is null in the FC case. As a consequence of this efficient entropy transport, a very large amount of heat per unit volume ($\rho T \delta S$) is fed to the mode, as T and ρ increase quickly with depth, leading to

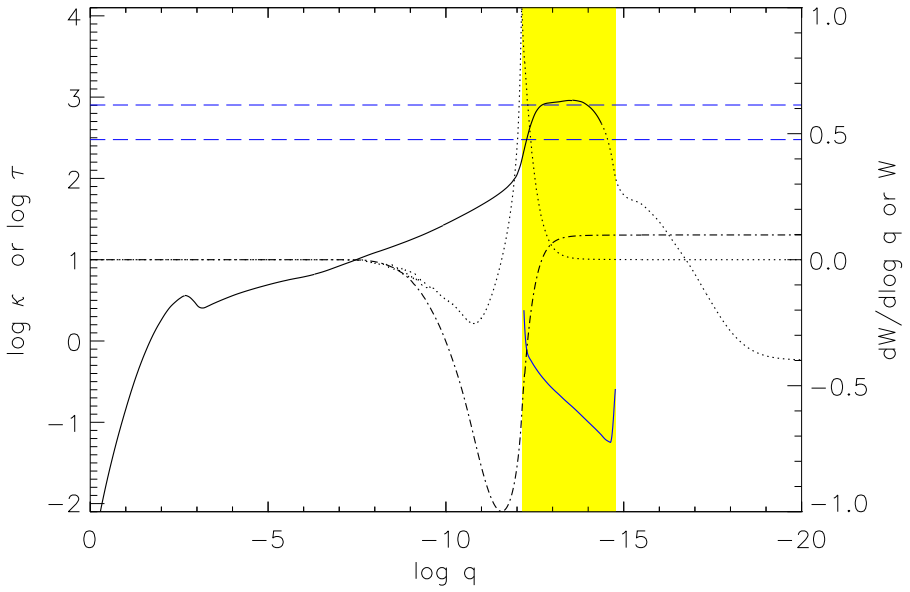

Figure 4. Similar to Fig. 2, but for a 0.54 $M_{\odot}$ V777 Her star at $\log g = 7.87$ and $T_{\rm eff} = 26,800$ K. This unstable model is close to the blue edge of the instability strip. The small opacity bump at $\log q \sim -2.5$ marks the transition zone between the carbon-oxygen core and the pure helium envelope above. The shaded (yellow) stripe gives the location and the extent of the convective zone, whereas the associated solid (blue) line gives the dynamical time scale in that convective zone. The two horizontal dashed (blue) lines indicate the range of typical pulsation periods observed in V777 Her stars (300−800 s). The convection time scale is much shorter than the pulsation periods. The work integral and its derivative are for a $l = 1$ $k = 15$ g-mode. Unlike the case of a pure κ-mechanism, the maximum of the driving does not occur at the maximum of the opacity bump, but at the base of the convection zone.

a large mechanical work driving the oscillations. Also, the temperature perturbation follows the same trend and phase as those followed by the entropy perturbation around the bottom of the convective zone. We can understand better this proportionality with the following thermodynamic relation

$$\frac{\delta S}{c_p} = \frac{\delta T}{T} + \nabla_{ad} \frac{\delta p}{p}, \tag{1}$$

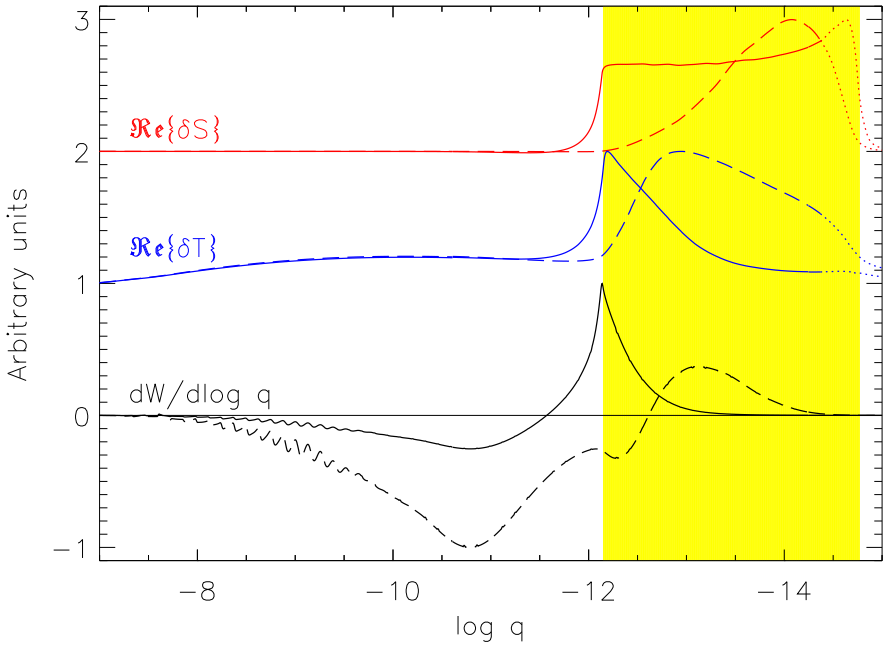

Figure 5. Zoom on the damping/driving layers and convection zone of the model described in Fig. 4. We compare the time dependent convection (TDC) treatment and the frozen convection (FC) approximation for that model. The real value of entropy perturbation δS (red), the real value of the temperature perturbation δT (blue), and the derivative of the work integral $dW/d\log q$ (black) are shown. The solid curves are used for TDC and the dashed curves for FC. All values are normalysed to $+1$ or -1, δS and δT are offset for readability.

where all quantities have their usual meaning. The rise of entropy around the bottom of the convection zone also increases the value of the pressure perturbation δp in that region with no direct effect on the mechanism describe here.

Knowing that δT follows the trend and the phase of δS, we can use the seminal Eddington relation of 1926, valid for quasi periodic oscillations,

$$W = \oint dt \int_0^M \delta T \frac{d\delta S}{dt} dm, \tag{2}$$

to understand differently the impact of the entropy transfer on the driving. The entropy along with temperature perturbations are transferred in phase to regions of higher density directly into the driving/damping layers. Work is then produced in large quantity: the mode turns unstable.

The immediate impact of the S-mechanism is that the blue edge is positioned at higher temperatures than would be the case for a typical κ-mechanism without convection or in the FC approximation. With the TDC, the driving potential of the partial ionization bump, lying over the driving/damping layer, is transferred into deeper regions of the star, making it unstable at higher effective temperatures than what the FC approximation predicts.

3. Conclusion

The excitation of GW Vir stars is tightly connected to the contents of carbon and oxygen in their envelope. Away from the red edge, the link between the spectroscopic parameters and the instability band is well understood. Quantitative astrophysics is even possible with nonadiabatic calculations on these stars (Quirion et al. 2008). It has also become clear that gravitational settling of C and O coming with the decrease of the wind velocity when the stars cool on the white dwarf track is responsible for the red edge of the instability strip.

We should concentrate future GW Vir observational efforts on the red edge side of the instability strip. The potential information to be gathered from the discovery of a cold GW Vir star (almost) turned into a DO white dwarf would be significant in the further understanding of both the wind-diffusion interaction and the spectral evolution of white dwarfs in general.

For the V777 Her stars, the understating of the interaction between pulsation and convection is on its way. With a firm grip on the blue edge via the S-mechanism, we can hope to reach a better understanding of the influence of the turbulent pressure on the red edge.

Further efforts should also be invested to get a better handle on the evolutionary connection that exists between the two types of stars. Evolutionary calculations involving diffusion and mass loss and adiabatic pulsation studies such as those pioneered by Fontaine & Brassard (2002) and Fontaine & Brassard (2005) and connecting the GW Vir and the V777 Her stars should be further developed.

Acknowledgments. P.-O. Q. is indebted to the members of the SOC for their kind invitation to present this review. He would also like to thank J. Christensen-Dalsgaard and G. Dogan for their interest in this work.

References

Beauchamp, A., Wesemael, F., Bergeron, P., Fontaine, G., Saffer, R. A., Liebert, J., & Brassard, P. 1999, ApJ, 516, 887

Brassard, P., & Fontaine, G. 1997, in White Dwarfs, ed. J. Isern, M. Hernanz, & E. Garcia-Berro (Dordrecht: Kluwer), 451

Chayer, P., Fontaine, G., & Pelletier, C. 1997, in ASSL Vol. 214: White dwarfs, 253

Dreizler, S., Heber, U., Napiwotzki, R., & Hagen, H. J. 1995, A&A, 303, L53

Dupret, M.-A. 2002, PhD thesis, Bull. Soc. Roy. Sc. Liège, 5-6, 249-445

Dupret, M.-A., Quirion, P.-O., Fontaine, G., Brassard, P., & Grigahcène, A. 2008, in Helioseismology, Asteroseismology and MHD Connections, ed. L. Gizon, Journal of Physics: Conference Series, in press

Eddington, A. S. 1926, The Internal Constitution of the Stars (Cambridge Univ. Press, Cambridge)

Fontaine, G., & Brassard, P. 2002, ApJ, 581, L33
Fontaine, G., & Brassard, P. 2005, in ASP Conf. Series 334, 14th European Workshop on White Dwarfs, ed. D. Koester and S. Moehler (San Francisco: ASP), 49
Gautschy, A., Ludwig, H.-G., & Freytag, B. 1996, A&A, 311, 493
Grigahcène, A., Dupret, M.-A., Gabriel, M., Garrido, R., & Scuflaire, R. 2005, A&A, 434, 1055
Quirion, P.-O., Fontaine, G., & Brassard, P. 2008, in Nonadiabatic Asteroseismology of GW Vir Stars, ed. L. Gizon, Journal of Physics: Conference Series, in press
Quirion, P.-O. 2007, Ph.D. thesis, Université de Montréal
Quirion, P.-O., Fontaine, G., & Brassard, P. 2007a, ApJS, 171, 219
Quirion, P.-O., Fontaine, G., & Brassard, P. 2007b, in ASP Conf. Ser. 372, 15th European Workshop on White Dwarfs, ed. Ralf Napiwotzki and Matthew R. Burleigh (San Francisco: ASP), 649
Tassoul, M., Fontaine, G., & Winget, D. E. 1990, ApJS, 72, 335
Unglaub, K., & Bues, I. 2000, A&A, 359, 1042
Unglaub, K., & Bues, I. 2001, A&A, 374, 570
Voss, B., Koester, D., Napiwotzki, R., Christlieb, N., & Reimers, D. 2007, A&A, 470, 1079
Werner, K. 2001, in Encyclopedia of Astronomy and Astrophysics, (London: IPP)
Werner, K., & Herwig, F. 2006, PASP, 118, 183